Available online at www.sciencedirect.com
SCIENCE DIRECT
Journal of Molecular Structure 795 (2006) 234–241
Journal of MOLECULAR STRUCTURE
www.elsevier.com/locate/molstruc

Electronic excitation in the benzonitrile dimer: The intermolecular structure in the S_0 and S_1 state determined by rotationally resolved electronic spectroscopy

Michael Schmitt [a,*], Marcel Böhm [a], Christian Ratzer [a], Swen Siegert [a], Marloes van Beek [b], W. Leo Meerts [b,*]

[a] Institut für Physikalische Chemie, Heinrich-Heine-Universität, D-40225 Düsseldorf, Germany
[b] Molecular- and Biophysics Group, Institute for Molecules and Materials, Radboud University Nijmegen, P.O. Box 9010, NL-6500 GL Nijmegen, The Netherlands

Received 24 January 2006; received in revised form 16 February 2006; accepted 16 February 2006
Available online 30 March 2006

Abstract

The rotationally resolved UV spectrum of the electronic origin of the benzonitrile dimer has been measured and analyzed using a genetic algorithm based fitting strategy. For the electronic ground state, a C_{2h} symmetric structure is found in which the permanent dipole moments of the benzonitrile monomers are aligned anti-parallel. The orientation of the transition dipole moment could be shown to be parallel to the orientation in the monomer moiety. The distance between the two monomer moieties decreases slightly upon electronic excitation and the symmetry of the benzonitrile dimer changes from C_{2h} in the electronic ground state to C_s in the electronically excited state. This break of symmetry is probably caused by the local excitation of only one benzonitrile moiety in the cluster due to the weak electronic coupling between the cluster moieties.

PACS: 33.15.Hp; 33.20.Lg; 33.20.Wr; 82.20.Wt; 31.15.Ar

Keywords: High-resolution UV spectroscopy; Structure determination; Excited state; Ab initio; Genetic algorithms

1. Introduction

Symmetrically bound homo-dimers raise the question if the electronic excitation is localized in one of the monomer moieties or if it is completely delocalized over both monomers. Closely related is the question, whether the complex conserves the inversion symmetry also in its excited state, leading to an exciton splitting, or if the symmetry is lost, leading to localized excitation in one monomer. Prototypes of these symmetrical homo-dimers are the benzoic acid dimer [1,2], the salicylic acid dimer [3,4], the 7-azaindole dimer [5], the 2-pyridone dimer [6–8], the *o*-cyanophenol dimer [9] and the benzonitrile dimer, investigated in this study. While for the 7-azaindole dimer and the 2-pyridone dimer delocalized excitation with an exciton splitting is found, the benzoic acid dimer, the fluorobenzoic acid dimer and the *o*-cyanophenol dimer show a local excitation in only one of the moieties. The strength of electronic coupling between two or more chromophores is crucial in exciton formation for energy harvesting or energy funneling devices in nature.

The benzonitrile dimer has been studied using laser induced fluorescence spectroscopy by Kobayashi et al. [10] On the basis of a rotational contour, they concluded that the structure of the benzonitrile dimer is planar. Takayanagi et al. investigated the relaxation of vibronically excited benzonitrile and the benzonitrile dimer by fluorescence dip spectroscopy [11]. While the monomer shows slow decay, no LIF signal for vibronically excited dimer bands could be detected, probably caused by a fast relaxation.

Determination of the cluster structure requires at first the knowledge of the monomer structures in both electronic states. The structure of the benzonitrile monomer has been investigated in great detail. The r_s-structure, in the electronic ground state has been determined using microwave spectroscopy of 10

* Corresponding authors.
E-mail addresses: mschmitt@uni-duesseldorf.de (M. Schmitt), leo.meerts@science.ru.nl (W.L. Meerts).
URLs: http://www.leomeerts.nl (M. Schmitt), http://www-public.rz.uni-duesseldorf.de/mschmitt (W.L. Meerts).

0022-2860/$ - see front matter © 2006 Elsevier B.V. All rights reserved.
doi:10.1016/j.molstruc.2006.02.036

different isotopomers by Casado et al. [12]. The rotational constants of benzonitrile in the S_1 state have been reported by Borst et al. [13] and by Helm et al. [14] Imhof et al. [15] performed a Franck–Condon analysis to determine structural changes upon electronic excitation.

Several van der Waals clusters of benzonitrile with Krypton [10], Argon [14] and Neon [16] have been investigated. In all of these cases, the noble gas atom is located above the aromatic plane, with a typical van der Waals distance of about 3.5 Å. The binary water cluster of benzonitrile has been studied in the electronic ground state using microwave spectroscopy by Melandri et al. [17] and in S_1 state using rotationally resolved electronic spectroscopy by Helm et al. [18] and Schäfer et al. [19]. They determined a cyclic structure of the water cluster with one water H-atom bound to the nitrogen of the nitrile group and the water oxygen atom bound to the ortho H-atom of the aromatic ring.

In the current paper, we will elucidate the intermolecular structure of the benzonitrile dimer in the ground state and the electronically excited state from a rotationally resolved electronic spectrum of the electronic origin.

2. Methods

2.1. Experimental

The experimental set-up for the rotationally resolved laser induced fluorescence (LIF) is described in detail elsewhere. [20] Briefly, it consists of a ring dye laser (Coherent 899–21) operated with Rhodamine 110, pumped with 7 W of the 515 nm line of a diode pumped cw Yb:YAG laser (ELS MonoDisk-515). The light is coupled into an external folded ring cavity (Spectra Physics) for second harmonic generation (SHG). The molecular beam is formed by expanding benzonitrile heated to 80 °C and seeded in 500 mbar of argon through a 100 μm hole into the vacuum. The molecular beam machine consists of three differentially pumped vacuum chambers, which are linearly connected by two skimmers (1 and 3 mm, respectively) in order to reduce the Doppler width. The molecular beam is crossed at right angles in the third chamber with the laser beam 360 mm downstream of the nozzle. The resulting fluorescence is collected perpendicularly to the plane defined by laser and molecular beam by an imaging optics set-up consisting of a concave mirror and two plano-convex lenses. The resulting Doppler width in this set-up is 15 MHz (FWHM). The integrated molecular fluorescence is detected by a photo-multiplier tube whose output is discriminated and digitized by a photon counter and transmitted to a PC for data recording and processing. The relative frequency is determined with a quasi confocal Fabry–Perot interferometer with a free spectral range (FSR) of 149.9434(56) MHz. The absolute frequency was determined by recording the iodine absorption spectrum and comparing the transitions to the tabulated lines [21].

2.2. The genetic algorithms

We used an automated fitting procedure for the rovibronic spectra, based on a genetic algorithm fit, which is described in detail in Refs. [16] and [22]. The GA library PGAPack version 1.0 is used, which can run on parallel processors [23]. For the simulation of the rovibronic spectra a rigid asymmetric rotor Hamiltonian was employed [24]

$$H = AP_a^2 + BP_b^2 + CP_c^2. \tag{1}$$

Here, the $P_g (g = a,b,c)$ are the components of the body fixed angular momentum operator, and A, B and C are the three rotational constants. The temperature dependence of the intensity is described by a two temperature model [25]

$$n(E, T_1, T_2, w) = e^{-E/kT_1} + we^{-E/kT_2} \tag{2}$$

where E is the energy of the lower state, k is the Boltzmann constant, w is a weighting factor, T_1 and T_2 are the two temperatures. The calculations were performed on 64 processors (Intel Itanium 2, 1.3 GHz) of an SGI Altix 3700 system and on 64 processors (Intel Xeon processors, 3.4 GHz) of a Linux cluster.

The cost function used to describe the quality of the fit is defined as $C_{fg} = 100(1 - F_{fg})$ with the fitness function F_{fg}

$$F_{fg} = \frac{(\boldsymbol{f}, \boldsymbol{g})}{\|\boldsymbol{f}\| \, \|\boldsymbol{g}\|}. \tag{3}$$

$\boldsymbol{f}$ and $\boldsymbol{g}$ represent the experimental and calculated spectra, respectively and the inner product $(\boldsymbol{f},\boldsymbol{g})$ is defined with the metric $\boldsymbol{W}$ as

$$(\boldsymbol{f}, \boldsymbol{g}) = \boldsymbol{f}^{\mathrm{T}} \boldsymbol{W} \boldsymbol{g}, \tag{4}$$

and the norm of $\boldsymbol{f}$ as $\|\boldsymbol{f}\| = \sqrt{(\boldsymbol{f},\boldsymbol{f})}$ and similar for $\boldsymbol{g}$. $\boldsymbol{W}$ has the matrix elements $W_{ij} = w(|j - i|) = w(r)$. For $w(r)$ we used a triangle function [22] with a width of the base of Δw:

$$w(r) = \begin{cases} 1 - \dfrac{|r|}{(1/2)\Delta w} & \text{for } |r| \le (1/2)\Delta w \\ 0 & \text{otherwise.} \end{cases} \tag{5}$$

In the first iterations, the value of Δw is chosen as about five times the linewidth in the spectrum. The final fit with a strongly narrowed search space for each parameter is performed using a base width of zero.

2.3. Ab initio calculations

The structure of the benzonitrile dimer in its electronic ground state has been optimized at the HF/6-31G(d,p) and MP2/6-31G(d,p) levels of theory and at the CIS/6-31G(d,p) level for the electronically excited S_1-state with the Gaussian 98 program package (Revision11) [26]. The SCF convergence criterion used throughout the calculations was an energy change below 10^{-8} Hartree, while the convergence criterion for the gradient optimization of the molecular geometry was $\partial E/\partial r < 1.5 \times 10^{-5}$ Hartree/Bohr and $\partial E/\partial \phi < 1.5 \times 10^{-5}$ Hartree/degrees, respectively. The harmonic vibrational frequencies were calculated, using the analytical second derivatives of the potential energy.

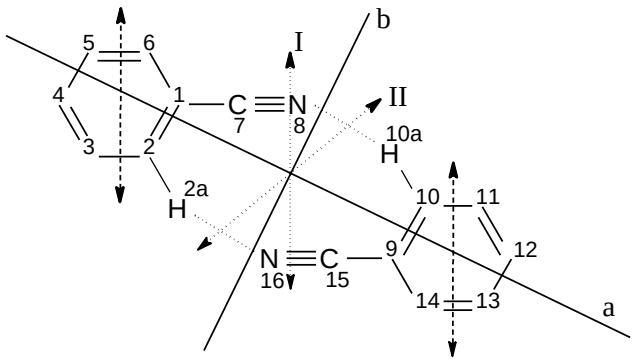

Fig. 1. Atomic numbering of the benzonitrile dimer and orientation of the inertial axes of the cluster. The dashed double arrows indicate the transition dipole moment orientation in each monomer moiety. The dotted double arrows (I and II) show the two possible orientations of the TDM in the cluster.

3. Results and discussion

Fig. 1 shows the atomic numbering and the orientation of the inertial axes of the benzonitrile dimer. Furthermore, the orientation of the transition dipole moment of the monomer moieties is shown. In the monomer inertial frame, they point along the *b*-axis. I and II designate two possible orientations of the transition dipole moment of the dimer. They will be discussed in detail below. The ground state of the benzonitrile dimer has C_{2h} symmetry, the first one-photon allowed transition can be classified in this point group as $S_1(^1B_u) \leftarrow S_0(^1A_g)$.

3.1. Assignment of the spectrum

Fig. 2 shows the rovibronic spectrum of the electronic origin of the benzonitrile dimer together with the best GA fit using the molecular parameters from Table 1. The lowest trace shows a zoomed part of the convoluted simulation along with the calculated stick spectrum. The electronic origin of the benzonitrile dimer is found at 36,420.10(1) cm^{-1}, which is 92.64 cm^{-1} red-shifted relative to the electronic origin of the monomer [13]. Thus, the stabilization energy of the cluster is higher in the electronically excited state.

The spectrum is fit using a rigid rotor Hamiltonian with a two temperature model. It is of mixed abc-type and consists of about 18,000 lines in a range of 55 GHz. At a rotational temperature of about 2.8 K more than 95 J states are populated with an intensity of at least 0.5% of the strongest transition in the spectrum. The rotational constants for both electronic states, the origin frequencies, the polar angles θ and ϕ, defining the orientation of the transition dipole moment in the inertial frame, and the Lorentzian contribution to a Voigt profile with 15 MHz Gaussian contribution are given in Table 1.

Comparison of the stick spectrum with its convolution using the experimental line widths immediately reveals, why a 'classical' fit with line position assignments is impossible for a molecular system of that size. Each 'line' in the experimental spectrum is composed of up to 40 single rovibronic transitions, in many cases of very similar intensities. Fig. 3 shows an expanded view of the simulated stick spectrum along with the convoluted spectrum using a Gaussian width of 15 MHz and a Lorentzian contribution of 10 MHz in the range −1500 to 0 MHz.

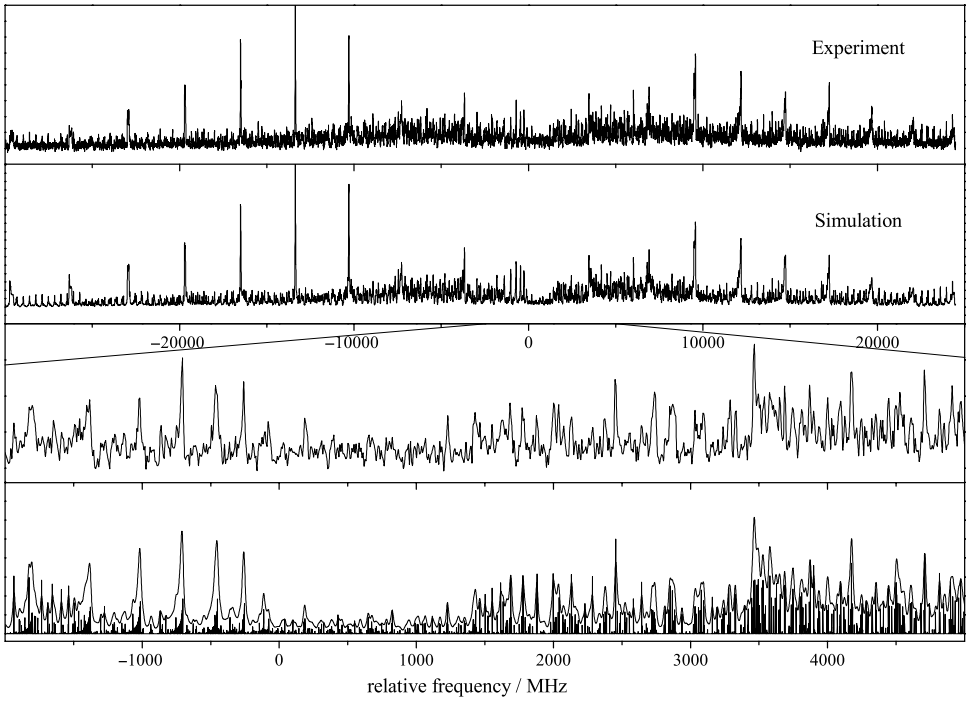

Fig. 2. Rovibronic spectrum of the electronic origin of the benzonitrile dimer at 36,420.10 cm^{-1}. The traces show the experimental spectrum, the simulated spectrum using the rotational constants from Table 1, a zoomed portion of the experimental spectrum and the zoomed simulation together with the stick spectrum.

Table 1
Molecular parameters of the electronic origin band of the benzonitrile dimer as obtained from the genetic algorithm fit

	Experiment	MP2	HF	CIS
A''/MHz	1610.99(17)	1654	1559	–
B''/MHz	187.48(7)	185	183	–
C''/MHz	168.12(7)	167	164	–
$\Delta I''$/μÅ^2	−3.2727	0	0	0
ν_0/cm^{-1}	36420.10(1)	–	–	–
ϕ/°	79.6(10)	–	–	90.0
θ/°	58.0(10)	–	–	57.9
$\Delta\nu$(Lorentz)/MHz	10(2)	–	–	–
ΔA/MHz	−28.08(10)	–	–	−20[a]
ΔB/MHz	−0.01(10)	–	–	0[a]
ΔC/MHz	−0.31(10)	–	–	0[a]
A'/MHz	1582.90(20)	–	–	1539
B'/MHz	187.47(12)	–	–	183
C'/MHz	168.12(12)	–	–	164
$\Delta I'$/μÅ^2	−3.4394	0	0	0

All ab initio calculations have been performed using the 6-31G(d,p) basis set. Standard deviations are given in parentheses.
[a] Rotational constants(HF) − rotational constants(CIS).

The Lorentzian contribution of 10(2) MHz as obtained from the GA fit corresponds to an excited state lifetime of 16(3) ns. The relative large uncertainty for the lifetime is also a consequence of the large number of overlapping lines.

The polar angles ϕ and θ in Table 1 are related to the components of the transition dipole moments (TDM) along the main inertia axes by:

$$\mu_a = \mu \sin\phi \cos\theta \qquad \mu_b = \mu \sin\phi \sin\theta \qquad \mu_c = \mu \cos\phi. \tag{6}$$

Since the squares of the TDM components are proportional to the observed intensities, the spectrum is of mainly b-type character (70%), with a smaller fraction of a-type (27%) and very litte c-type contribution (3%).

Both the quite small negative inertial defect (−3.2727 μÅ^2 for the S_0 and −3.4394 μÅ^2 for the S_1 state) and the very small c-type (out-of-plane) contribution to the TDM points to a planar structure in both electronic states. A really non-planar cluster structure with two heavy moieties would have a much larger inertial defect. The deviation of the inertial defect from zero can be attributed to out-of-plane zero-point vibrational contributions from large amplitude vibrations of the floppy cluster. The inertial defect of the planar benzonitrile monomer, which has no large amplitude motions amounts to 0.085 μÅ^2.

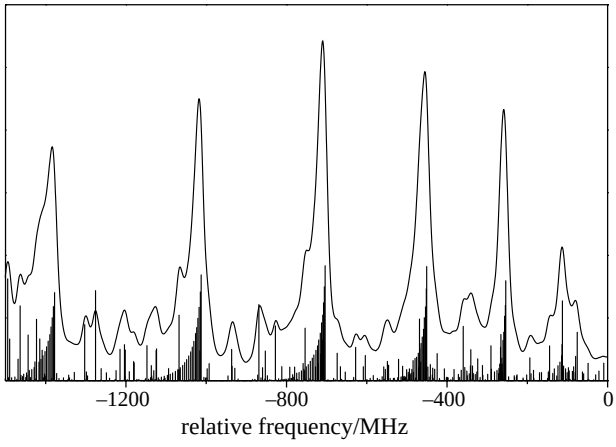

Fig. 3. Expanded view of the simulated stick spectrum along with the convolution using a Gaussian width of 15 MHz and a Lorentzian contribution of 10 MHz in the range −1500 to 0 MHz.

For comparison the rotational constants computed for the optimized structure at the MP2/6-31G(d,p) level for the ground state are also shown. Deviations are smaller than 3% for all rotational constants. For the electronically excited state we estimated the changes of the rotational constants from the difference of a CIS/6-31G(d,p) and a HF/6-31G(d,p) calculation. Given the same level of approximation for both levels, the changes of the calculated constants reproduce the observed changes of the rotational constants very well, while of course the absolute values for ground and excited states are far off. The orientation of the TDM calculated at the CIS level of theory agrees well with the experimental value.

We also calculated the harmonic vibrational frequencies of the cluster in the electronic ground state at the MP2/6-31G(d,p) level and in the electronically excited state at CIS/6-31G(d,p) level of theory. The lowest vibration at 10.3 cm^{-1} (8.6 in the S_1) is the out-of-plane butterfly motion of the two aromatic rings. Three out-of-plane intermolecular motions are found below 41 cm^{-1} in the electronic ground state and below 31.8 cm^{-1} in the electronically excited state, accounting for the non-zero inertial defect of the cluster. Since, all vibrational frequencies of the out-of-plane vibrations in the excited state are smaller than in the ground state the vibrationally induced inertial defect is larger in the S_1 state, cf. Table 2. All six intermolecular modes and their description are summarized in Table 2.

3.2. Determination of the structure, transition dipole moment orientation and comparison to the results of ab initio calculations

A first approach to the change of the cluster structure upon electronic excitation can be made using the center of mass (CM) distance of the monomer moieties in the cluster as has been shown for the phenol dimer by Connell et al. [27].

Table 2
Approximate despriptions of the intermolecular vibrations and vibrational frequencies of the benzonitrile dimer in the S_0 and S_1 state

Description		Frequency/cm^{-1}	
		S_0	S_1
Butterfly	oop	10.3	8.6
Twist	oop	32.0	29.6
Gearing	ip	37.8	36.4
Wagging	oop	41.0	31.8
Gearing	ip	59.3	46.8
Stretch	ip	71.7	58.3

The CM distance R of the two monomer moieties is given by

$$R = \sqrt{\frac{\sum_g I_g^{\text{Dimer}} - \sum_g I_g^{\text{Donor}} - \sum_g I_g^{\text{Acceptor}}}{2\mu}} \quad (7)$$

where μ is the reduced mass of donor and acceptor, and the I_g are the respective moments of inertia, described by their superscripts, which are calculated from the experimental rotational constants.

The first column in Table 3 gives the CM distances of the two monomer moieties, calculated for the electronic ground and excited states from Eq. (7), using the rotational constants from Ref. [12] for the ground state and from Ref. [13] for the electronically excited state. A slight reduction of the CM distance of 2.81 pm upon electronic excitation is found, which will be discussed below.

The program pKrFit [28] was used to determine the intermolecular structure of the benzonitrile dimer in the S_0 and S_1-state from the rotational constants, given in Table 1. pKrFit uses a gradient-based χ^2 minimizer as well as a GA based global optimizer [29]. While the gradient method is much faster, its main disadvantage is the possibility of being trapped in a local minimum, depending on the starting geometry for the fit. The genetic algorithm based fit varies the geometry parameters between given limits and leads generally to the global minimum. The GA library [23] was used in minimization mode and directly used the least square (χ^2) value as cost function.

Prior to the fit of the intermolecular dimer structure, the structural parameters for the monomer moieties have to be determined. For the ground state, we took the r_s-geometry from Casado et al. [12] for both monomer moieties (first column in Table 4). This monomer structure (in the following called model I) results from a classical Kraitchman analysis [30]. Subsequently, we fitted the benzonitrile monomer pseudo-r_s-structure [28] to the rotational constants of the ten isotopomers given in Ref. [12] (second column in Table 4 in the following called model II).

For the electronically excited state much less information is available. Since for the excited state only one isotopomer of benzonitrile has been measured with high-resolution electronic spectroscopy, we had to use a model with many constraints. All CC bond lengths in the aromatic ring are treated equally and are fit, furthermore the C_1 distance is fit, the C_7N_8 distance is kept fixed at the ground state value, and all CH bond lengths are kept fixed at a value of 107.1 pm which is a typical value for excited state aromatic CH bonds. The average CC bond length in the aromatic ring determined in this way is 142.8 pm, the C_1C_7 distance was determined to 142.7 pm. Comparing the structures of ground and excited state, one thus finds an overall expansion of the aromatic ring, and a reduction in the distance of the cyano group from the aromatic ring. Using the so obtained structures, the distances of the nitrogen atom from the CM can be calculated for both electronic states. The distance d(CM–N_8) is found to be larger in the excited state (316 pm), than in the ground state (314 pm).

Both monomer geometries were then kept fixed in the fit of the intermolecular geometry of the dimer. The CH–N bond lengths in the dimer using model I and II for the monomer moieties differ slightly. For monomer model I we obtain a value of 236.46(5) pm, for model II of 235.80(13) pm. This gives a rough estimate of systematic errors introduced by using different models for the monomer moieties. The other fitted parameters are given in Table 4. The CM distance is then calculated for both fitted dimer geometries (model I and model II) and compared to the CM distance, obtained from application of Eq. (7) (cf. Table 3). Within the uncertainty, the CM distances are equal, demonstrating the applicability of the chosen models for the ground state.

While for the electronic ground state only the question arises about the applicability of the assumption of unchanged

Table 3
Center of mass distance (pm) of the benzonitrile moieties in the ground and electronically excited state of the cluster

	CM distance[a]	Fit1[b]	Fit2[c]	Fit3[d]	Fit4[e]
S_0	649.81	649.45	649.61		
S_1	647.00			648.59	647.08

[a] Calculated from equation (7).
[b] Calculated from the S_0-structure in column 1 of Table 4.
[c] Calculated from the S_0-structure in column 2 of Table 4.
[d] Calculated from the S_1-structure in column 3 of Table 4.
[e] Calculated from the S_1-structure in column 4 of Table 4.

Table 4
Structural parameters of the benzonitrile dimer

	S_0[a]	S_0[b]	S_1[c]	S_1[d]
$d(N_8H_{10a})$	236.46(5)	235.80(13)	231.1(3)	235.5(2)
$\alpha(N_8H_{10a}C_{10})$	162.20(17)	162.30(56)	162.45(18)	160.20(19)
$\alpha(C_7N_8H_{10a})$	138.76(14)	138.36(19)	138.89(48)	138.84(15)
$d(C_1C_2)$	138.76(5)	137.67(23)	138.76(5)	142.8(1)
$d(C_2C_3)$	139.56(4)	139.20(21)	139.56(4)	142.8(1)
$d(C_3C_4)$	139.74(4)	140.24(4)	139.74(4)	142.8(1)
$d(C_2H_{2a})$	108.03(6)	108.24(13)	108.03(6)	107.1[e]
$d(C_3H_{3a})$	108.22(3)	108.17(16)	108.22(3)	107.1[e]
$d(C_4H_{4a})$	107.96(4)	108.03(15)	107.96(4)	107.1[e]
$d(C_1C_7)$	145.09(6)	145.18(4)	145.09(6)	142.7(1)
$d(C_7N_8)$	115.81(2)	115.81(10)	115.81(2)	115.81[e]
$d(C_9C_{10})$	138.76(5)	137.67(23)	142.8(1)	142.8(1)
$d(C_{10}C_{11})$	139.56(4)	139.20(21)	142.8(1)	142.8(1)
$d(C_{11}C_{12})$	139.74(4)	140.24(4)	142.8(1)	142.8(1)
$d(C_9H_{9a})$	108.03(6)	108.24(13)	107.1[e]	107.1[e]
$d(C_{10}H_{10a})$	108.22(3)	108.17(16)	107.1[e]	107.1[e]
$d(C_{11}H_{11a})$	107.96(4)	108.03(15)	107.1[e]	107.1[e]
$d(C_9C_{15})$	145.09(6)	145.18(4)	142.7(1)	142.7(1)
$d(C_{15}N_{16})$	115.81(2)	115.81(10)	115.81[e]	115.81[e]

The first three lines show the fitted intermolecular parameters. The other distances and angles are obtained from a fit to the monomer rotational constants of Casado et al. [12] for the ground state and of Borst et al. [13] for the excited state, cf. text.
[a] r_s-monomer geometry from Ref. [12].
[b] pseudo-r_s-monomer geometry fitted to the rotational constants from Ref. [12].
[c] One monomer moiety excited.
[d] Both monomer moieties excited.
[e] Kept fixed.

monomer geometries in the cluster, the excited state possesses a much more difficult problem. In homo-dimers like the benzonitrile dimer, the excitation might be localized in one of the monomer moieties or it might be delocalized over both. We performed two different fits that are presented in columns 3 and 4 of Table 4. The first fit assumes local excitation, which was modeled by using the ground state structure parameters for one moiety and the excited state structure for the other moiety. The second fit was performed with the S_1 state structure for both monomers. The results of the fit are given in Table 4. Of course, the intermolecular geometry depends strongly on the chosen model for the excited state. In case of local excitation, the distance between N_8 and H_{10a} is smaller (231.1 pm) than in the case of delocalized excitation (235.5 pm). Nevertheless, both models show nearly the same CM distance (cf. Table 3), so that no discrimination between the two models can be made on the basis of the CM distances.

The experimentally determined structural parameters are compared to the ab initio structure in Table 5. For both the monomer geometries in the dimer and the intermolecular geometry a very close agreement between the MP2 calculation and the experimental values is found. This fact again shows, that the assumption of unchanged monomer geometries in the cluster is appropriate. The MP2 calculations yield a dipole moment of exactly 0 Debye, what can be expected for the perfectly anti-parallel aligned dipole moments of the monomer moieties.

The geometry changes upon electronic excitation are compared to the differences of the respective coordinates of the HF and the CIS calculations. The N_8H_{10a} distance calculated on CIS level is 3.2 pm shorter than calculated at the HF level, while the two intermolecular angles $\alpha(N_8H_{10a}C_{10})$ and $\alpha(C_7N_8H_{10a})$ nearly stay the same (cf. Table 5). For the excited state a dipole moment of 0.25 Debye is found on CIS level, showing the inequality of the two monomers. The good coincidence between the experimental values for the intramolecular structure parameters and the calculated ones has to be traced back to a fortuitous cancellation of errors, due to the same level of approximation between the CIS and the HF calculations. Also the intramolecular structure changes upon electronic excitation have been reported in Table 5. They point to a completely localized excitation in one of the benzonitrile rings.

Table 5
Comparison of of the experimentally determined structural parameters of the benzonitrile dimer with ab initio calculated values

	S_0	MP2	S_1	$\Delta(S_0$–$S_1)$	HF–CIS
$d(N_8H_{10a})$	236.46(5)	238.71	231.1(3)	5.36	3.2
$\alpha(N_8H_{10a}C_{10})$	162.20(17)	158.51	162.45(18)	−0.25	0.2
$\alpha(C_7N_8H_{10a})$	138.76(14)	141.14	138.89(48)	−0.13	1.1
$d(C_1C_2)$	138.76(5)	140.55	142.8(1)	+4.0	+5.0
$d(C_2C_3)$	139.56(4)	139.18	142.8(1)	+3.2	−1.4
$d(C_3C_4)$	139.74(4)	139.72	142.8(1)	+3.1	+4.0
$d(C_2H_{2a})$	108.03(6)	108.48	107.1[a]	−0.9	−0.2
$d(C_3H_{3a})$	108.22(3)	108.55	107.1[a]	−1.1	−0.2
$d(C_4H_{4a})$	107.96(4)	108.60	107.1[a]	−0.9	−0.2
$d(C_1C_7)$	145.09(6)	143.47	142.7(1)	−2.4	−5.1
$d(C_7N_8)$	115.81(2)	116.32	115.81[a]	0	+1.1
$d(C_9C_{10})$	138.76(5)	140.55	138.76(5)	0	0
$d(C_{10}C_{11})$	139.56(4)	139.18	139.56(4)	0	0
$d(C_{11}C_{12})$	139.74(4)	139.72	139.74(4)	0	0
$d(C_9H_{9a})$	108.03(6)	108.48	108.03(6)	0	0
$d(C_{10}H_{10a})$	108.22(3)	108.55	108.22(3)	0	0
$d(C_{11}H_{11a})$	107.96(4)	108.60	107.96(4)	0	0
$d(C_9C_{15})$	145.09(6)	143.47	145.09(6)	0	0
$d(C_{15}N_{16})$	115.81(2)	116.32	115.81(2)	0	0

[a] Kept fixed.

The angle of the transition dipole moment with the inertial a-axis upon electronic excitation of the benzonitrile dimer is 58.0° (cf. Table 1). Since, we only know the projection on the axis, the transition dipole might be oriented in two ways, as shown in Fig. 1. Orientation I is nearly parallel to the orientation of the transition dipole in the benzonitrile monomer moieties. Under the assumption of unchanged TDM orientation upon cluster formation we favor orientation I over orientation II. The results of the ab initio CIS/6-31G(d,p) calculations for the planar TDM orientation angle θ of 57.9° agree perfectly with the experimental value a of 58°. Since the out-of-plane contribution to the TDM orientation is due to zero-point motions, the angle ϕ is calculated at ab initio level to be 90°, while experimentally we find an angle of 79.6°. The very good numerical agreement between the calculations and the experimental value is due to a favourable cancellation of errors. A more reliable method for TDM calulations like multi reference CI would require a much larger basis set.

4. Conclusions

We determined geometry parameters of the benzonitrile dimer in the ground and electronically excited state from rotational constants, that were obtained by rotationally resolved electronic spectroscopy. In the ground state, a C_{2h} symmetric cluster is found in agreement with the predictions from ab initio MP2/6-31G(d,p) calculations. The main reason for the cluster stabilization is the dipole–dipole interaction, which leads to completely anti-parallel orientations in the ground state. Since the experimentally determined orientation of the transition dipole moment is reproduced at the CIS level, it can be expected that the excited state dipole moment is also calculated correctly. We found an excited state dipole moment of 0.25 Debye and therefore propose a local excitation for the electronically excited state in one of the benzonitrile monomer moieties, leading to a non-symmetric structure. The larger dipole moment in the excited state of benzonitrile leads to a slightly stronger interaction that is reflected in the shorter CM distance in the excited state. Nevertheless, since no vibronic bands of the benzonitrile dimer are observed, a delocalized excitation cannot be completely excluded. In this case, the observed electronic transition would be only one component of an exciton split origin transition $(S_1(^1B_u) \leftarrow S_0(^1A_g))$. The other (one-photon forbidden) component would be $S_2(^1A_g) \leftarrow S_0(^1A_g)$. The indexing of the excited state does not imply an energetic ordering in this case. A straightforward

distinction between these two possibilities can only be made on the basis of assigned vibronic bands in the excitation spectrum of the dimer. Nevertheless, on the basis of the experimentally observed shortening of the hydrogen bond, which is reproduced by the CIS calculations (cf. Table 5) we prefer the mechanism of local excitation with a change of symmetry from C_{2h} in the electronic ground state to C_s in the electronically excited state. What causes the excitation in some doubly hydrogen bonded homo-dimers to be delocalized as in the cases of the 7-azaindole dimer and the pyridone dimer, and in other cases, like the *o*-cyanophenol dimer, the benzoic acid dimer and the benzonitrile dimer to be localized in one of the cluster moieties? Obviously, the strength of electronic coupling between the cluster constituents has to be very different. In both 7-azaindole and pyridone a second tautomer exists, which can be mutually formed in the respective dimer upon electronic excitation. The electronic interaction between the chromophors is partially mediated via a partial through-bond mechanism. No second tautomer with a comparable energy exists for *o*-cyanophenol, benzoic acid or benzonitrile. Therefore, the purely through-space electronic interaction is much weaker in these cases leading to localized excitation in one of the monomers.

Acknowledgements

This work was made possible by the support of the Deutsche Forschungsgemeinschaft (SFB 663 project A2). The authors like to thank the National Computer Facilities of the Netherlands Organization of Scientific Research (NWO) for a grant on the Dutch supercomputing facility SARA. This work was also supported by the Netherlands Organization for Scientific Research and the Deutsche Forschungsgemeinschaft in the framework of the NWO-DFG bilateral programme.

References

[1] D.E. Poeltl, J.K. McVey, Excited-state dynamics of hydrogen-bonded dimers of benzoic acid, J. Chem. Phys. 80 (1984) 1801–1811.
[2] K. Remmers, W.L. Meerts, I. Ozier, Proton tunneling in the benzoic acid dimer studied by high reolution uv spectroscopy, J. Chem. Phys. 112 (2000) 10890–10894.
[3] P.B. Bisht, H. Petek, K. Yoshihara, Excited state enol–keto tautomerization in salicylic acid: a supersonic free jet study, J. Chem. Phys. 103 (1995) 5290–5307.
[4] T. Yahagi, A. Fujii, T. Ebata, N. Mikami, Infrared spectroscopy of the OH stretching vibrations of jet-cooled salicylic acid and its dimer in s_0 and s_1, J. Phys. Chem. A 105 (2001) 10673–10680.
[5] K. Sakota, H. Sekiya, Excited-state double-proton transfer in the 7-azaindole dimer in the gas phase. 1. Evidence of complete localization in the lowest excited electronic state of asymmetric isotopomers, J. Phys. Chem. A 109 (1995) 2718–2721.
[6] A. Held, D.W. Pratt, The 2-pyridone dimer, a model cis peptide. Gas-phase structure, J. Am. Chem. Soc. 112 (1990) 8629–8630.
[7] A. Held, D.W. Pratt, Hydrogen bonding in the symmetry-equivalent c_{2h} dimer of 2-pyridone in its s_0 and s_1 electronic states. Effect of deuterium substitution, J. Chem. Phys. 96 (1992) 4869–4876.
[8] A. Müller, F. Talbot, S. Leutwyler, S_1/S_2 exciton splitting in the $(2\text{-pyridone})_2$ dimer, J. Chem. Phys. 116 (2002) 2836–2847.
[9] F. Lahmani, M. Broquier, A. Zehnacker-Rentien, The *o*-cyanophenol dimer as studied by laser-induced fluorescence and ir fluorescence dip spectroscopy: a study of a symmetrical double hydrogen bond, Chem. Phys. Lett. 337-348 (2002) 354.
[10] T. Kobayashi, K. Honma, O. Kajimoto, S. Tsuchiya, Benzonitrile and its van der waals complexes studies in a free jet. (I) the lif spectra and the structure, J. Chem. Phys. 322 (1987) 1111–1117.
[11] M. Takayagani, I. Hanazaki, Fluorescence-dip and stimulated-emission-pumping laser-induced-fluorescence spectra of van der waals molecules containing benzonitrile, J. Opt. Soc. Am B 7 (1990) 1898–1904.
[12] J. Casado, L. Nygaard, G.O. Sørensen, Microwave spectra of isotopic benzonitriles—refined molecular structure of benzonitrile, J. Mol. Struct. 8 (1971) 211–224.
[13] D.R. Borst, T.M. Korter, D.W. Pratt, On the additivity of bond dipole moments. Stark effect studies of the rotationally resolved electronic spectra of aniline, benzonitrile and aminibenzonitrile, Chem. Phys. Lett. 350 (2001) 485–490.
[14] R.M. Helm, H.-P. Vogel, H.J. Neusser, Highly resolved UV spectroscopy: structure of s_1 benzonitrile and benzonitrile–argon by correlation automated rotational fitting, Chem. Phys. Lett. 270 (1997) 285–291.
[15] P. Imhof, D. Krügler, K. Kleinermanns B.R., Geometry change of simple aromatics upon electronic excitation obtained from Franck–Condon fits of dispersed fluorescence spectra, J. Chem. Phys. 121 (1999) 2598–2610.
[16] W.L. Meerts, M. Schmitt, G. Groenenboom, New applications of the genetic algorithm for the interpretation of high resolution spectra, Can. J. Chem. 82 (2004) 804–819.
[17] S. Melandri, D. Consalvo, W. Caminati, P.G. Favero, Hydrogen bonding, structure, and dynamics of benzonitrile–water, J. Chem. Phys. 111 (9) (1999) 3874–3879.
[18] R.M. Helm, H.P. Vogel, H.J. Neusser, V. Storm, D. Consalvo, H. Dreizler, Combined high resolution UV and microwave results: structure of the benzonitrile–water complex, Z. Naturforsch. 52 (1997) 655–664.
[19] M. Schäfer, D. Borst, D.W. Pratt, K. Brendel, Tunnelling splittings in the high resolution microwave and uv spectra of the benzonitrile–water complex: modelling the internal motion in its s_0 and s_1 states, Mol. Phys. 100 (2002) 3553–3562.
[20] M. Schmitt, J. Küpper, D. Spangenberg, A. Westphal, Determination of the structures and barriers to hindered internal rotation of the phenol–methanol cluster in the s_0 and s_1 state, Chem. Phys. 254 (2000) 349–361.
[21] S. Gerstenkorn, P. Luc, Atlas Du Spectre D'absorption De la Molécule D'iode 14,800–20,000 cm^{-1}, CNRS, Paris, 1986.
[22] J.A. Hageman, R. Wehrens, R. de Gelder, W.L. Meerts, L.M.C. Buydens, Direct determination of molecular constants from rovibronic spectra with genetic algorithms, J. Chem. Phys. 113 (2000) 7955–7962.
[23] D. Levine, PGAPack V1.0, PgaPack can be obtained via anonymous (1996). ftp available from: ftp://ftp.mcs.anl.gov/pub/pgapack/pgapack.tar.z
[24] H.C. Allen, P.C. Cross, Molecular Vib-Rotors, Wiley, New York, 1963.
[25] Y.R. Wu, D.H. Levy, Determination of the geometry of deuterated tryptamine by rotationally resolved electronic spectroscopy, J. Chem. Phys. 91 (1989) 5278–5284.
[26] M.J. Frisch, G.W. Trucks, H.B. Schlegel, G.E. Scuseria, M.A. Robb, J.R. Cheeseman, V.G. Zakrzewski, J.A. Montgomery, Jr., R.E. Stratmann, J.C. Burant, S. Dapprich, J.M. Millam, A.D. Daniels, K.N. Kudin, M.C. Strain, O. Farkas, J. Tomasi, V. Barone, M. Cossi, R. Cammi, B. Mennucci, C. Pomelli, C. Adamo, S. Clifford, J. Ochterski, G.A. Petersson, P.Y. Ayala, Q. Cui, K. Morokuma, P. Salvador, J.J. Dannenberg, D.K. Malick, A.D. Rabuck, K. Raghavachari, J.B. Foresman, J. Cioslowski, J.V. Ortiz, A.G. Baboul, B.B. Stefanov, G. Liu, A. Liashenko, P. Piskorz, I. Komaromi, R. Gomperts, R.L. Martin, D.J. Fox, T. Keith, M.A. Al-Laham, C.Y. Peng, A. Nanayakkara, M. Challacombe, P.M.W. Gill, B. Johnson, W. Chen, M.W. Wong, J. Andres, C. Gonzalez, M. Head-Gordon, E.S. Replogle, J.A. Pople, GAUSSIAN 98, revision a.11, GAUSSIAN, Inc., Pittsburgh, PA (2001).

[27] L.L. Connell, S.M. Ohline, P.W. Joireman, T.C. Corcoran, P.M. Felker, Rotational coherence spectroscopy and structure of phenol dimer, J. Chem. Phys. 96 (1992) 2585–2593.
[28] C. Ratzer, J. Küpper, D. Spangenberg, M. Schmitt, The structure of phenol in the s_1-state determined by high resolution UV-spectroscopy, Chem. Phys. 283 (2002) 153–169.
[29] M. Schmitt, D. Krügler, M. Böhm, C. Ratzer, V. Bednarska, I. Kalkman, W.L. Meerts, A genetic algorithm based determination of the ground and excited ^1l_b state structure and the orientation of the transition dipole moment of benzimidazole, Phys. Chem. Chem. Phys. 8 (2006) 228–235.
[30] J. Kraitchman, Determination of molecular structure from microwave spectroscopic data, Am. J. Phys. 21 (1953) 17.